Available online at www.sciencedirect.com
ScienceDirect
ELSEVIER
International Journal of Pharmaceutics 330 (2007) 183–194
INTERNATIONAL JOURNAL OF PHARMACEUTICS
www.elsevier.com/locate/ijpharm

Pharmaceutical Nanotechnology

Photodynamic ultradeformable liposomes: Design and characterization

J. Montanari [a], A.P. Perez [a], F. Di Salvo [b], V. Diz [b], R. Barnadas [c,d], L. Dicelio [b], F. Doctorovich [b], M.J. Morilla [a], E.L. Romero [a,*]

[a] *Laboratorio de Diseño de Estrategias de Targeting de Drogas (LDTD), Departamento de Ciencia y Tecnología, Universidad Nacional de Quilmes, Roque Saenz Peña 180, Bernal B1876BXD, Buenos Aires, Argentina*
[b] *Departamento de Química Inorgánica, Analítica y Química Física/INQUIMAE-CONICET, Facultad de Ciencias Exactas y Naturales, Universidad de Buenos Aires, Ciudad Universitaria, Pabellon II, Argentina*
[c] *Centre de Estudis Biofísics, Universitat Autónoma de Barcelona, 08193 Cerdanyola, Catalunya, Spain*
[d] *Departament de Físicaquímica, Facultat de Farmácia, Universitat de Barcelona, Av. Joan XXIII, s/n 08028 Barcelona, Catalunya, Spain*

Received 30 August 2006; received in revised form 2 November 2006; accepted 3 November 2006
Available online 11 November 2006

Abstract

Hydrophobic ([tetrakis(2,4-dimetil-3-pentyloxi)-phthalocyaninate]zinc(II)) (ZnPc) and hydrophilic ([tetrakis(*N*,*N*,*N*-trimethylammoniumetoxi)-phthalocyaninate]zinc(II) tetraiodide) (ZnPcMet) phthalocyanines were synthesized and loaded in ultradeformable liposomes (UDL) of soybean phosphatidylcholine and sodium cholate (6:1, w/w, ratio), resulting 100 nm mean size vesicles of negative Zeta potential, with encapsulation efficiencies of 85 and 53%, enthalpy of phase transition of 5.33 and 158 J/mmol for ZnPc and ZnPcMet, respectively, indicating their deep and moderate partition into UD matrices. Matrix elasticity of UDL-phthalocyanines resulted 28-fold greater than that of non-UDL, leaking only 25% of its inner aqueous content after passage through a nanoporous barrier versus 100% leakage for non-UDL. UDL-ZnPc made ZnPc soluble in aqueous buffer while kept the monomeric state, rendering singlet oxygen quantum yield (Φ_Δ) similar to that obtained in ethanol (0.61), whereas UDL-ZnPcMet had a four-fold higher Φ_Δ than that of free ZnPcMet (0.21). Free phthalocyanines were non-toxic at 1 and 10 μM, both in dark or upon irradiation at 15 J/cm^2 on Vero and J-774 cells (MTT assay). Only liposomal ZnPc at 10 μM was toxic for J-774 cells under both conditions. Aditionally, endo-lysosomal confinement of the HPTS dye was kept after irradiation at 15 J/cm^2 in the presence of UDL-phtalocyanines. This could lead to improve effects of singlet oxygen against intra-vesicular pathogen targets inside the endo-lysosomal system.

Keywords: Ultradeformable liposomes; Phthalocyanines

1. Introduction

The outermost layer of epidermis known as *stratum corneum* (SC) blocks drug permeation and penetration across the intact skin, and it hampers percutaneous absorption. Because of that, topical treatment of cutaneous diseases represent an important challenge (Blank and Scheuplein, 1969; Scheuplein and Blank, 1971; Menon, 2002) since drugs can not always be delivered in therapeutic doses nor with the adequate selectivity (Cevc, 2004). In general terms, the calculated maximal transdermal flux of a drug with molecular weight under 1 kDa at 1 mmol/cm^2 (the maximal drug concentration on the skin surface is limited by solubility and toxicity), results extremely low, in the order of pM/h/cm^2 (Cevc and Blume, 2004). This could be the reason why, in case of cutaneous leishmaniasis, topical treatments have to be applied to open lesions that have lost their SC layer, and are less successful in lesions where absorption is hindered by epithelial thickening (Blum et al., 2004).

Another limitation of topical treatments arises from the fact that penetration depth and selectivity depend on drug's physicochemical properties and not on the excipients (creams, gels, lotions) (Weiner and Lieb, 1998). In spite of the attempts done to improve delivery across the SC employing particulate controlled release systems (PCRS) such as niosomes, liposomes, micro and nanoparticles, PCRS could only penetrate the SC across the hydrophilic nanochannels existent between or inside the queratinocytes clusters (Schatzlein and Cevc, 1998; Cevc and Blume, 2004). Since nanochannels posses an effective diameter several fold below those of PCRS, their high size and/or absence of elasticity impair the penetration. For instance, in the dry envi-

* Corresponding author. Tel.: +54 1143657100; fax: +54 1143657132.
E-mail address: elromero@unq.edu.ar (E.L. Romero).

0378-5173/$ – see front matter © 2006 Elsevier B.V. All rights reserved.
doi:10.1016/j.ijpharm.2006.11.015

ronment of the SC surface, conventional liposomes coalesce and fuse, only functioning as reservoirs for sustained drug release (Abraham and Downing, 1990; Hofland et al., 1995).

Ultradeformable liposomes (UDL) (Cevc and Blume, 1992; Cevc et al., 1993; Cevc, 1995, 1996; Honeywell-Nguyen and Bouwstra, 2005) are vesicles with new useful features as compared to conventional liposomes. UDL posses elastic energy (κ) in the order of ambient thermal energy (kT), which is nearly 20-fold lower than that of conventional liposomes. The meta stable lipid matrices of UDL, consistent of mixtures of conventional phospholipids and edge activators such as surfactants (bile salts) or co-solvents (ethanol), are capable of experiencing strong spontaneous fluctuation at room temperature (Cevc, 1995). Remarkably, UDL make use of the transepithelial water gradient as driving force to penetrate across the skin. The resultant force ($F = \Pi r_v^2 \times 10^5$ Pa, where r_v is the vesicle ratio) in the order of 10^{11} to 10^{12} N, is sufficient to impulse the locomotion of the UDL across the nanochannels of the SC, without collapsing nor coalesce (Barry, 2001; Cevc and Blume, 2003; Verma et al., 2003).

On the other hand, photodynamic therapy (PDT), which is an emerging new bimodal strategy that involves the combination of visible light and a photosensitizer, is used for treating a large variety of pathologies such as psoriasis, cancer, dysplastic and infectious diseases (Ochsner, 1997) including cutaneous leishmaniasis (Abok et al., 1988; Hongcharu et al., 2000; Lang et al., 2001; Stojiljkovic et al., 2001; Enk et al., 2003; Gardlo et al., 2003; Dutta et al., 2005). Hydrophobicity is one of the most important factors that modulate the phototherapeutic activity of a photosensitizer (Krieg et al., 2003). However, the same as for any other active principle, it is expected that their phototherapeutic activity (particularly if dependent on the hydrophilic/hydrophobic balance) can be strongly modified with respect to the free forms when loaded in nano-PCRS; those modifications will depend on the nano-PCRS design and structure, which can be tuned to improve the *in vivo* performance.

In the present work, we describe the design and characterization of UDL loaded with two different dyes, a hydrophobic (ZnPc) and a hydrophilic (ZnPcMet) phthalocyanine derivatives. In the example of cutaneous leishmaniasis, earlier and therefore more effective topical treatments can not be applied because of impairment of the intact SC. This proposed photodynamic UDL could be applied at less developed stages, in spite of the barrier properties of intact epidermis.

2. Materials and methods

2.1. Materials

3-Nitrophthalonitrile, *N*,*N*-dimethylethanolamine, 2,4-dimethyl-3-pentanol, DBU, anhydrous zinc(II) acetate, methyl iodide, anhydrous chloroform, 1-pentanol, *N*,*N*-diethyl-1-4 nitrosoaniline and 1,3-diphenylisobenzofuran (DPBF) were purchased from Aldrich. Imidazol was from Riedel de Häen, NaH and THF from Merck and Methylene Blue from Química Bonaerense. Tetra-*t*-butylphthalocyaninate zinc(II) was synthesized by Fernandez et al. (1995). Pentanol was dried with CaH_2 and stored with molecular sives 3 Å under nitrogen atmosphere. THF was dried with Na/benzophenone and distilled before use. Soybean phosphatidylcholine (SPC) (phospholipon 90 G, purity >90%) was a gift from Phospholipid/Natterman, Germany. Sodium cholate (NaChol), thiazolyl blue tetrazolium bromide (MTT) and Sephadex G-50 were purchased from Sigma. The fluorophore 8-hydroxypyrene-1,3,6-trisulfonic acid (HPTS) and the quencher *p*-xylene-bis-pyridinium bromide (DPX) were purchased from Molecular Probes (Eugene, OR, USA). RPMI 1640 culture medium, antibiotics and foetal calf serum (FCS) were purchased from PAA-GmbH. Other reagents were analytic grade from Anedra, Argentina.

2.2. Phthalocyanines preparation

2.2.1. [Tetrakis(2,4-dimetil-3-pentyloxi)-phthalocyaninate]zinc(II)

This hydrophobic zinc(II)-phthalocyanine (Fig. 1), ZnPc, MW = 1052, was synthesized according to Liu et al. (2004) with a yield of 87%.

2.2.2. [Tetrakis(N,N,N-trimethylammoniumetoxi)-phthalocyaninate]zinc(II) tetraiodide

Hydrophilic zinc(II)-phthalocyanine (Fig. 1), ZnPcMet, MW = 1492.5, was synthesized based on Liu et al. (2004) and De Filippis et al. (2000). 3-(*N*,*N*-Dimethyletoxi)-phthalonitrile

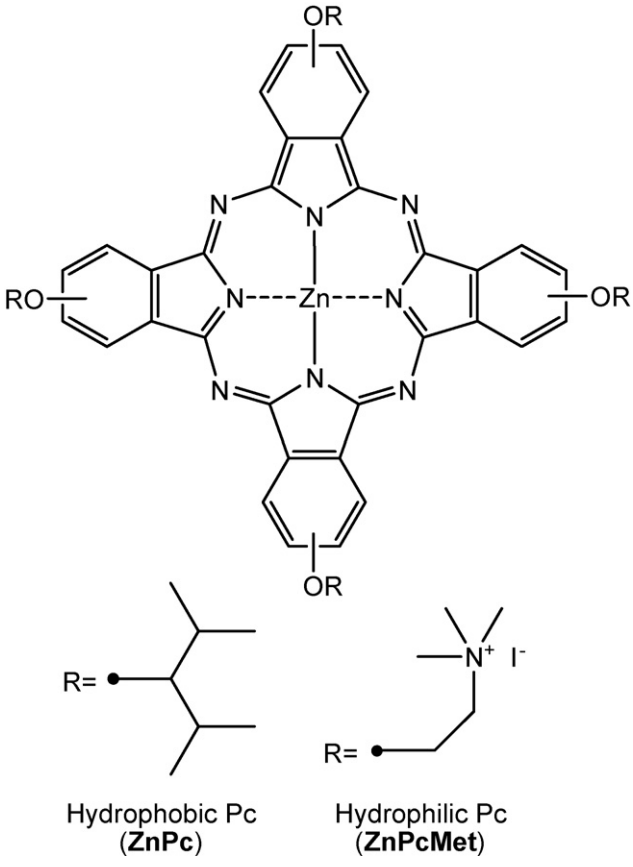

Fig. 1. Chemical structure of hydrophobic and hydrophilic phthalocyanines.

precursor was synthesized through a modification of the patent JP9077731 (Shigeo et al., 1997). The [tetrakis(*N*,*N*,-dimethylaminetoxi)-phthalocyaninate]zinc(II) (neutral precursor for ZnPcMet, MW = 924.5) was obtained from the above mentioned phthalonitrile (50.0 mg, 0.023 mmol) solubilized in dry pentanol 3 ml) in the presence of DBU (35.0 mg, 0.23 mmol) and Zn(II) acetate (10.2 mg, 0.06 mmol) by refluxing during 8 h. The phthalocyanine was isolated from the crude mixture through protonation of the amino groups by treatment with aqueous acetic acid, washing the aqueous solution with several solvents. After basification with K_2CO_3, extraction of the neutral compound with Et_2O and slow precipitation of the pure product by evaporation of the solvent, the green solid was obtained (49.9 mg, 0.054 mmol) with a yield of 90%.

(a) ^{1}H NMR (500 MHz, $CHCl_3$-*d*1) (ppm) 8.1 (t, 1H), 7.7 (dd, 1H), 7.5 (dd 1H), 5.1 (t, 2H), 3.3 (t, 2H), 2.6 (s, 6H); (b) ^{13}C NMR (125 MHz, $CHCl_3$-*d*1) (ppm) 120–115, 68.4, 46.4, 32.6, 22.6; (c) ESI-MS CH_2Cl_2) $[M+H]^+$: $m/z = 925.49$ and $[M+Na]^+$: $m/z = 947.49$; (d) UV–vis (etOH) $\varepsilon = 3.1 \times 10^4\ M^{-1}\ cm^{-1}$ ($\lambda_{max} = 694.5$ nm).

For ZnPcMet synthesis, 50.0 mg (0.053 mmol) of its precursor dissolved in $CHCl_3$ were treated with excess of methyl iodide (151.8 mg, 1.07 mmol) in the presence of DBU (8.1 mg, 0.053 mmol). Then the mixture was refluxed for 5 h. After cooling at room temperature, the green precipitate was isolated by centrifugation, washed with cool $CHCl_3$ and ether. Yield: 82% (101.1 mg, 0.067 mmol).

(a) ^{1}H NMR (500 MHz, DMSO-*d*6) (ppm) 8.1 (t, 1H), 7.96 (m, 2H), 5.3 and 5.5 (broad t, 2H), 4.1 and 4.3 (broad t, 2H), 2.4, 3.2 and 3.3 (s, 9H); (b) ^{13}C NMR (125 MHz, DMSO-*d*6) (ppm) 114–120, 64.6, 54.8, 53.8, 48.1, 27.5, 25.6, 21.7, 19.4; (c) ESI-MS (MeOH/H_2O) $[M-2CH_3+3I]^+$: $m/z = 1081.6$, $[M-H-I+NaI]^{2+}$ and $m/2z = 693.57$, $[M-CH_3]^{3+}$: $m/3z = 323.34$, $[M-4I]^{4+}$: $m/4z = 246.33$; (d) UV–vis (buffer Tris) $\varepsilon = 2.2 \times 10^4\ M^{-1}\ cm^{-1}$ ($\lambda_{max} = 702.5$ nm).

2.3. Ultradeformable liposomes preparation

Ultradeformable liposomes composed of SPC and NaChol at 6:1 (w/w) ratio, were prepared by mixing lipids from $CHCl_3$ and $CHCl_3$:CH_3OH (1:1, v/v) solutions, respectively, that were further rotary evaporated at 40 °C in round bottom flask until organic solvent elimination. The thin lipid film was flushed with N_2, and hydrated with 10 mM Tris–HCl buffer plus 0.9% (w/v) NaCl, pH 7.4 (Tris buffer), up to a final concentration of around 43 mg SPC/ml. The resultant liposomal suspension was sonicated (45 min with a bath type sonicator 80 W, 40 kHz) and extruded 15 times through three stacked 0.2, 0.1 and 0.1 μm pore size polycarbonate filters using a 100 ml Thermobarrel extruder (Northern Lipids, Canada).

Basically, the same steps stated above were followed to incorporate both phthalocyanines into UDL, excepting that ZnPc were co-solubilized in organic solution with lipids (2 mg ZnPc/g SPC) to prepared UDL-ZnPc and ZnPcMet was dissolved in the Tris buffer (2.8 mg ZnPcMet/g SPC) to hydrate the thin lipid film to obtain UDL-ZnPcMet.

Non-incorporated ZnPcMet was separated from UDL-ZnPcMet by gel permeation chromatography in a Shepadex G-50 column using minicolumn centrifugation method (Fry et al., 1978). Due to its low aqueous solubility, no further separation of free ZnPc from UDL-ZnPc was required.

Conventional, non-ultradeformable, liposomes (without NaChol) were prepared by the same procedure.

2.4. Physico-chemical characterization of liposomal phthalocyanines

The phthalocyanine/phospholipid ratio (mg/g) of each liposomal preparation was determined by phospholipid and phthalocyanine quantitation. Liposomal phospholipids were quantified by a colorimetric phosphate micro assay (Bötcher et al., 1961) whereas liposomal phthalocyanines were quantified by absorbance upon complete disruption of one volume of liposomal suspension in 10 volumes of ethanol. Absorbance was measured at λ_{max} of the Q band (707 and 702 nm for ZnPc and ZnPcMet, respectively) in an UV–vis Shimadzu spectrophotometer UV-160 A. Calibration curves prepared in ethanol used to quantify each phthalocyanine resulted linear in concentration range of 0.6–4.7 μM for ZnPc and 1.2–7.5 μM for ZnPcMet, with correlation coefficients exceeding 0.998.

Mean particle size of each liposomal preparation was determined by dynamic light scattering with Autosizer 2C (Malvern) just after preparation and followed through time to determine stability with a Microtrac Ultrafine Particle Analyzer. Zeta potential was determined with a Zetasizer 4 (Malvern). Negative staining electron microscopy images of liposomes upon uranyl acetate staining were obtained with a TEM Jeon 1210, 120 kV, equipped with EDS analyzer LINK QX 2000.

2.5. Differential scanning calorimetry

Temperature of phase transitions (T_m) and associated change of enthalpy (ΔH_{cal}) of liposomes were determined by differential scanning calorimetry, from −50 to 30 °C at 10 °C/min rate, in a Mettler Toledo DSC 822.

2.6. Deformability test

The flux of 3.5 ml of UDL, UDL-ZnPc, UDL-ZnPcMet and conventional liposomes driven by an external pressure of 0.8 MPa through two stacked 50 nm pore size membranes (Thermobarrel extruder) was determined to test deformability (Cevc, 1995). Extruded volume was collected every minute along 15 min and phospholipid was determined for each fraction. Both phthalocyanines were quantified in the total volume recovered.

Additionally, the retention degree (RD) of liposomal inner aqueous phase after passage through the nanoporous barrier was determined. To that aim, the fluorophore/quencher pair HPTS/DPX was incorporated into conventional liposomes and UDL, basically as stated in Section 2.3, excepting that the lipid films were hydrated with a solution of 35 mM HPTS and 50 mM DPX in 10 mM Tris–HCl buffer (pH 7.4). After extrusion, non-incorporated HPTS and DPX were eliminated by gel permeation

in Sephadex G-50, as stated above. Fluorescence emission intensity of HPTS (λ_{exc}, 465 nm; λ_{em}, 516 nm) was monitored in a ISS K2 multifrequency phase fluorometer, before and after passage through the 50 nm barrier, driven by 0.8 MPa for UDL and 2.5 MPa for conventional liposomes.

RD was calculated as: $100 - [(I_{50} - I_o)/I_T] \times 100$, where I_{50} was the fluorescence intensity after passage through 50 nm, I_o the fluorescence intensity before passage and I_T was the total intensity obtained after addition of Triton X-100 at 0.1% (v/v).

2.7. Photochemical characterization of free and liposomal phthalocyanines

2.7.1. Absorption spectroscopy and fluorescence emission

Electronic absorption spectra were obtained in a Shimadzu UV-3101 PC spectrophotometer using ethanol, Tris buffer or empty UDL as reference.

Fluorescence emission spectra were monitored in a QuantaMaster Model QM-1 PTI spectrofluorometer. The emission spectra were registered at 610 nm (Q band) as the excitation wavelength and were recorded between 630 and 800 nm, a cut-off filter was used to prevent the excitation beam from reaching the detector (Schott RG 630).

Emission and absorption spectra of liposomal phthalocyanines were corrected for light scattering by subtracting the spectra from empty liposomes.

2.7.2. Fluorescence quantum yield (Φ_F)

Fluorescence quantum yields (Φ_F) for air saturated solutions of free and liposomal phthalocyanines were determined by comparison with tetra-*t*-butylphthalocyaninato zinc(II) in toluene ($\Phi_F = 0.33$) as reference (Fernandez et al., 1996). The quantum yields were calculated as usual with Eq. (1):

$$\Phi_F^S = \Phi_F^R \frac{I_S}{I_R} \frac{(1 - 10^{-A_R})}{(1 - 10^{-A_S})} \left(\frac{n_S}{n_R}\right)^2 \quad (1)$$

where R and S refer to the reference and sample, respectively, I the integrated area under the emission spectrum, A the solution absorbance at the excitation wavelength and $(n_S/n_R)^2$ stands for the refractive index correction. In buffer solutions and in dilute liposomal media the refractive index was assumed to be the same as water. Optical densities were set below 0.1 A.U. at the excitation wavelength (610 nm).

2.7.3. Singlet oxygen quantum yield (Φ_Δ)

Singlet oxygen photoproduction (O_2, $^1\Delta_g$) was quantified by steady state irradiation in the presence of DPBF for ZnPc in ethanol solution, for ZnPcMet and for liposomal phthalocyanines in the presence of imidazol (8 mM) and *N*,*N*-diethyl-4-nitrosoaniline (40–50 μM) in Tris buffer. Suspensions were saturated with air and irradiated under continuous stirring in 10 mm path length optical cells. The bleaching of nitrosoaniline was followed spectrophotometrically at 440 nm (Shimatzu UV-160 spectrophometer) as a function of time and quantum yields were calculated using Methylene Blue as a reference ($\Phi_\Delta = 0.56$ in buffer and ethanol) (Wilkinson et al., 1995).

Chemical monitor bleaching rates were used as usual to calculate the singlet oxygen photogeneration rates (Kraljic and El Mohsni, 1978; Lagorio et al., 1993). Polychromatic irradiation was performed using a projector lamp (Philips 7748SEHJ, 24V-250W) and a cut-off filter at 630 nm (Schott, RG 630). Sample and reference were irradiated within the same wavelength interval λ_1–λ_2, and Φ_Δ was calculated according to Eq. (2):

$$\Phi_\Delta^S = \Phi_\Delta^R \frac{r^S}{r^R} \frac{\int_{\lambda_1}^{\lambda_2} I_o(\lambda)(1 - 10^{-A^R(\lambda)})\,d\lambda}{\int_{\lambda_1}^{\lambda_2} I_o(\lambda)(1 - 10^{-A^S(\lambda)})\,d\lambda} \quad (2)$$

where r is the singlet oxygen photogeneration rate and the superscripts S and R stand for sample and reference, respectively, A the absorbance at the irradiation wavelength and $I_o(\lambda)$ is the incident spectral photon flow (mol/s/nm). When the irradiation wavelength range is narrow, the incident intensity varies smoothly with wavelength and sample and reference have overlapping spectra, I_o may be approximated by a constant value which may be drawn out of the integrals and cancelled.

Singlet oxygen quantum yield of the reference was measured in liposomal solutions and compared against the same experiments in buffer solutions. As the same results of the singlet oxygen photogeneration rate were obtained, the liposomal media do not change the (O_2, $^1\Delta_g$) radiative decay constant.

2.8. Cytotoxicity assay

Cell viability, upon incubation with free or liposomal phthalocyanines in the dark or upon sun or lamp irradiation, was measured as mitochondrial dehydrogenase activity employing a tetrazolium salt (MTT) on Vero and the murine macrophage-like cell line J-774.

Cells maintained at 37 °C with 5% CO_2, in RPMI 1640 medium supplemented with 10% heat-inactivated foetal calf serum, 2 mM glutamine, 100 UI/ml penicillin and 100 μg/ml streptomycin and amphotericin, were seeded at a density of 5×10^4 cells/well in 96-well flat bottom microplates.

Culture medium of nearly confluent cell layers was replaced by 100 μl of medium containing 1 or 10 μM of free or liposomal phthalocyanines (between 0.8 and 20 mM of phospholipids). Empty UDL at 18 mM of phospholipid were used as control. Because of its poor water solubility, free ZnPc was dissolved in dimethylsulfoxide (DMSO) and diluted in culture medium at 1 and 10 μM, resulting less than 1% (v/v) DMSO final concentration. Upon 18 h at 37 °C incubation in the dark, suspensions were removed, replaced by fresh RPMI medium and cells were exposed to two different light sources: direct sunlight along 15 min (light dose of 15 J/cm^2 at $\lambda = 600$–650 nm measured by Radiometer Laser Mate Q, Coherent; coincident with the reported value of media solar radiation on Earth surface) (Uriarte Cantolla, 2003) or irradiated with a 6 V–20 W halogen lamp of fluorescence microscope along 30 min to render 15 J/cm^2. The same procedure was carried out without irradiation for determining dark toxicity.

After treatments, cellular cultures were incubated for 24 h at 37 °C, media were removed and replaced by fresh RPMI medium containing at 0.5 mg/ml of MTT. Upon 3 h incubation, MTT

solution was removed, the insoluble formazan crystals were dissolved in DMSO and absorbance was measured at 570 nm in a microplate reader.

2.9. Liposomal cell uptake and fate of liposomal HPTS upon irradiation

Cell uptake and intracellular fate of the fluorescent dye HPTS loaded in UDL alone (UDL-HPTS/DPX) or together with each phthalocyanine (UDL-HPTS/DPX-ZnPc and UDL-HPTS/DPX-ZnPcMet prepared as stated in Sections 2.3 and 2.6), was followed upon incubation with Vero and J-774 cells by fluorescence microscopy.

Liposomal cell uptake was determined on both cell types grown to nearly confluence on rounded coverslips in 24-well plates. Upon 5, 10 or 15 min incubation at 37 °C with UDL-HPTS/DPX in the dark, liposomal suspensions were removed, cells were washed, and coverslips were mounted on a fluorescence microscope. Cell-associated fluorescence of HPTS was monitored for 45 min with a Nikon Alphaphot 2 YS2 fluorescence microscope.

Additionally, cells incubated 45 min in the dark with UDL-HPTS/DPX-ZnPc or UDL-HPTS/DPX-ZnPcMet, as stated before, were fixed with methanol for 10 min and the emission of HPTS and phthalocyanines were registered with a confocal laser microscopy Olympus FV300, under excitation with an Ar 488 nm and HeNe 633 nm laser, respectively.

The effect of phthalocyanines and irradiation on the fate of liposomal HPTS, was determined in both cell types grown as stated before in two 24-well plates upon incubation with UDL-HPTS/DPX, UDL-HPTS/DPX-ZnPc or UDL-HPTS/DPX-ZnPcMet for 45 min. After incubation, cells were washed and one plate was placed under microscope light irradiation up to a total energy dose of 15 J/cm^2, while the other plate remained in the dark and sequential photographs were taken along 30 min.

3. Results

3.1. Physico-chemical characterization of liposomal phthalocyanines

Results depicted in Table 1 show that the phthalocyanine/phospholipid ratio for UDL-ZnPc resulted to be almost twice of that obtained for UDL-ZnPcMet, whereas the encapsulation efficiency was 85 and 53%, respectively.

Table 1
Physico-chemical characterization

	UDL-ZnPc	UDL-ZnPcMet
Phthalocyanine/SPC[a]	1.73 ± 0.53	0.95 ± 0.36
E.E. (%)[b]	85.55 ± 14.92	53.06 ± 4.78
Mean diameter (nm)	99.9 ± 1.2	112.7 ± 1.4
Polydispersity index	0.105	0.134
Zeta potential (mV)	−36.7 ± 3.8	−26.3 ± 3.1

[a] Ratio expressed as mg of phthalocyanine per gram of phospholipids. Mean ± D.S. (n = 3).
[b] E.E.: encapsulation efficiency (%) of phthalocyanine. Mean ± D.S. (n = 3).

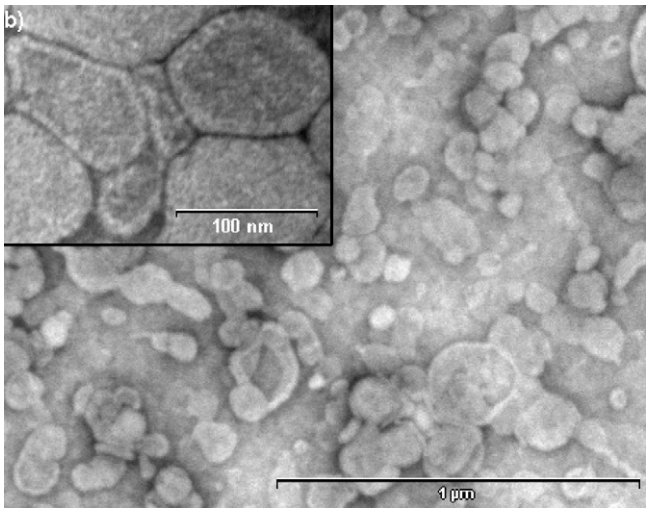

Fig. 2. Transmission electron microscopy following negative staining (20,000×). (Inset) Detailed picture, where unilamellarity and size of vesicles can be seen (80,000×).

The preparation method rendered empty UDL of 100 nm size with unimodal distribution and negative value of Zeta potential. As shown in Table 1, phthalocyanine incorporation did not modify the mean sizes in both cases, remaining in the order of 100 nm (with narrow size distribution as judged by their low polydispersity index) nor the Zeta potential. Additionally, all liposomal suspensions showed good colloidal stability after storage at 4 °C for at least 33 days; with no significant changes of size distribution neither polydispersity.

Fig. 2 depicts electron micrographs of liposomal ZnPc, which appear as unimellar spherical shaped vesicles. In agreement with light scattering size measurements, liposomes presented a uniform size of 100 nm. No differences were found between both liposomal phthalocyanines.

3.2. Calorimetric measurements

Differential scanning calorimetry was used to determine the effect of the incorporation of both phthalocyanines in the thermotropic behaviour of the liposomal bilayers. Thermotropic profiles of aqueous suspensions of all liposomal bilayers, show two endothermic peaks, one close to 0 °C corresponding to fusion of aqueous medium and other, below 0 °C (Fig. 3). Thermodynamic parameters corresponding to each thermogram are shown in Table 2. The transition temperature obtained showed no significant differences due to incorporation of both phthalo-

Table 2
Effect of incorporation of phthalocyanines on thermodynamic parameters of ultradeformable matrices

Sample	T_m[a] (°C)	ΔH_{cal}[b] (J/mmol phospholipid)
UDL	−22.81	−210.47
UDL-ZnPcMet	−22.87	−158
UDL-ZnPc	−22.22	−5.33

[a] Temperature corresponding to the maximum of the calorimetric peak.
[b] Calorimetric enthalpy calculated as area under the curve.

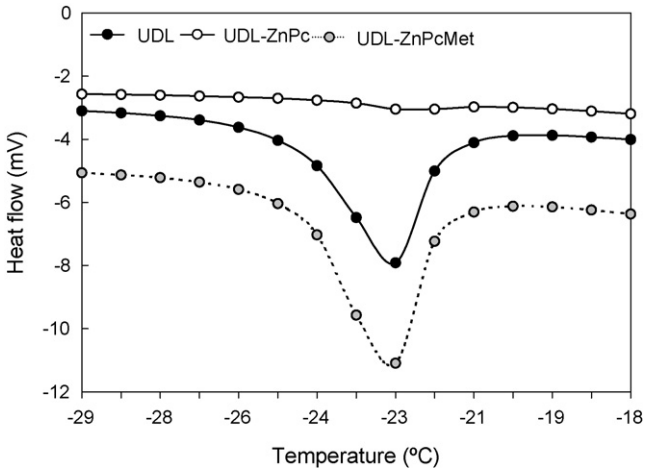

Fig. 3. Differential scaning calorimetry of empty and phthalocyanine ultradeformable liposomes.

cyanines with regard to empty UDL. However, the incorporation of ZnPc into liposomes strongly decreased the phase transition enthalpy, whereas the incorporation of ZnPcMet also affected this parameter. These results indicate that hydrophobic ZnPc, as specked, was incorporated into the bilayers, therefore producing significative changes in the bilayer organization, decreasing its cooperativity (Postigo et al., 2004). On the other hand, this effect was weaker for the hydrophilic ZnPcMet, probably because of its lower interaction with membranes, mostly remaining soluble in the aqueous inner phase of liposomes.

3.3. Deformability test

3.3.1. Liposomal deformability

Liposomal phospholipids passage across 50 nm pore size membrane under an external pressure of 0.8 MPa is shown in Fig. 4. The profiles of all the ultradeformable compositions (empty UDL and both phthalocyanine incorporated liposomes) showed a biphasic mode, characterized by a fast passage during the first 3 min (60% recovered phospholipids) followed by a slower passage the rest 12 min when nearly 90% of the phospholipids were recovered. Conversely, no phospholipid passage

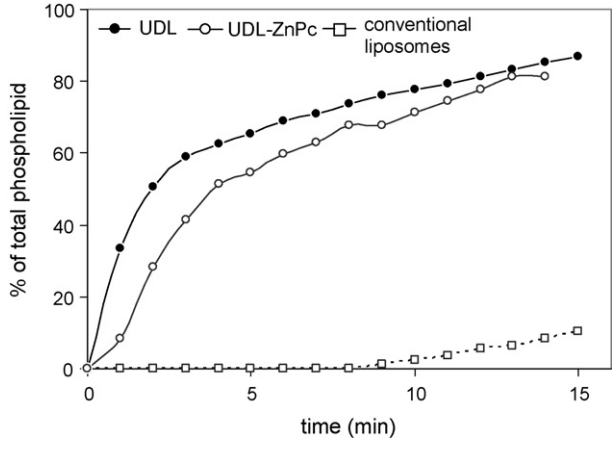

Fig. 4. Profile of phospholipid passage through 50 nm pore size vs. time.

was registered for conventional liposomes during the first 10 min with only 15% recovered phospholipids at the end of the 15 min.

The elasticity of liposome bilayers (D) was calculated according to van den Bergh et al. (2001), where $D = J(r_v/r_p)^2$. The flux (J) of liposomes through a nanoporous barrier was calculated as the area under the curve from the plot of liposomal phospholipids passage versus time, r_v the vesicle size after passage and r_p is the membrane pore diameter. The results indicated that empty UDL and both liposomal phthalocyanines had the same elasticity ($D = 283$) and resulted 28-fold more elastic than conventional liposomes ($D = 10$).

Liposomes prepared with higher initial phthalocyanines/phospholipid ratios, rendered calculated elasticity significantly lower (data not shown).

3.3.2. Retention degree of aqueous content (RD)

The fluorophore/quencher pair HPTS/DPX was incorporated into UDL and conventional liposomes in order to measure the RD of aqueous medium. HPTS is a membrane impermeant water-soluble fluorescent that is quenched when co-encapsulated with DPX. Dequenching occurs if HPTS is released to the external medium upon liposomal leakage or disruption. Fluorescence intensity of released HPTS was used to calculate the RD of liposomes under mechanical stress such as passage across the narrow 50 nm diameter nanochannels. To perform the assay under similar conditions, a pressure of 2.5 MPa on conventional liposomes was used to render the same phospholipid flux than that of UDL at 0.8 MPa.

The results showed that 76% of HPTS was retained into UDL while only 7.5% of HPTS was retained into conventional liposomes after passage through the barrier.

The post-stress quantification of ZnPc showed not relevant lost from liposomes; for ZnPcMet only a minor quantity was lost, in coincidence with leakage of HPTS.

3.4. Spectroscopic characterization

Absorption spectra of both phthalocyanines in homogeneous media (ethanol or buffer) and incorporated in liposomes are shown in Fig. 5. Neither significant wavelength shifts nor relevant modifications in shape were observed for free ZnPc (in ethanol) and for both phthalocyanines incorporated in liposomes. Absorption maxima were found at 707 nm both for ZnPc in ethanol and incorporated in liposomes, and 702 nm for ZnPcMet in liposomes, and the spectra were characteristic of the monomeric state of the reported phthalocyanines (Wilkinson et al., 1995; Strassert et al., 2003). No effect of concentration was observed in absorption spectra of ZnPc in the studied concentration range in ethanol (1×10^{-8} to 1×10^{-6} M), neither in liposomes (1×10^{-6} to 2×10^{-6} M). ZnPcMet is highly soluble in water but aggregation was evidenced by deviations from the Lambert–Beer law in the studied concentration range (1×10^{-8} to 1×10^{-6} M). Its absorption spectrum in buffer showed an important dimer band at 650 nm, as shown in Fig. 5. This situation is reverted when the phthalocyanine was incorporated into liposomes, the monomer band at 701 nm was enhanced and the dimer absorption band at 650 nm becomes negligible.

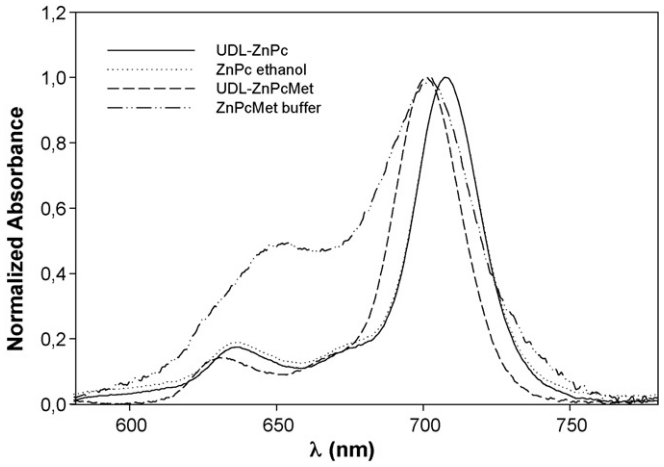

Fig. 5. Normalized absorption spectra of ZnPc in ethanol, ZnPcMet in buffer, UDL-ZnPc and UDL-ZnPcMet.

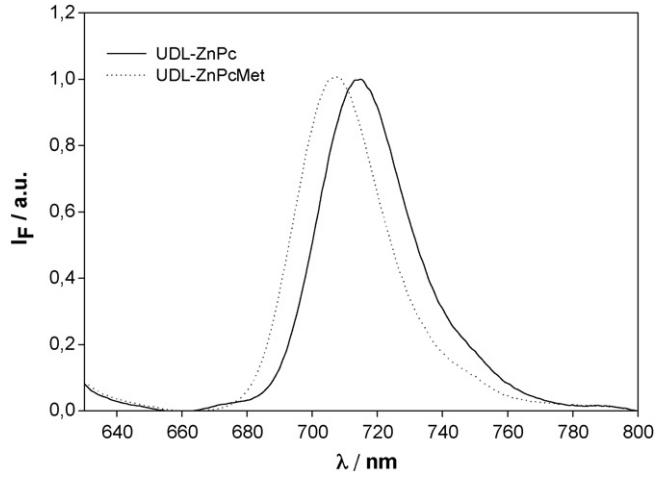

Fig. 6. Normalized emission spectra of ZnPc in ethanol, ZnPcMet in buffer, UDL-ZnPc and UDL-ZnPcMet.

The fluorescence emission spectra of phthalocyanines incorporated in liposomes are shown in Fig. 6. For both phthalocyanines, in solution and in liposomes and at increasing concentration, neither significant wavelength shifts nor relevant modifications in shape were observed, denoting that the monomer is the only fluorescent species.

The fluorescence quantum yields (Φ_F) and singlet oxygen quantum yield (Φ_Δ) were the same for ZnPc in ethanol and both phthalocyanines incorporated in liposomes (Table 3). For ZnPcMet, both Φ_F and Φ_Δ were lower in buffer solution than in liposomes, indicating aggregation in the homogeneous solution.

These results suggest that both phthalocyanines were incorporated into ultradeformable liposomes in monomeric state.

3.5. Cytotoxicity assay

The effect of free or liposomal phthalocyanines, either in the dark or after lamp or sun irradiation, on Vero and J-774 cells viability was measured by the MTT assay.

Viability of both cell lines was not affected by empty UDL. Similarly, Vero cells were not affected by neither free nor liposomal phthalocyanines up to 10 μM (of phthalocyanines) in the dark or upon irradiation (data not shown). Viability was only reduced in the dark at high doses, such as 100 μM (data not shown).

On the other hand, J-774 cells were not affected by free phthalocyanines; however, UDL-ZnPc at 10 μM reduced cell viability to 25%, both in the dark or after irradiation (Fig. 7).

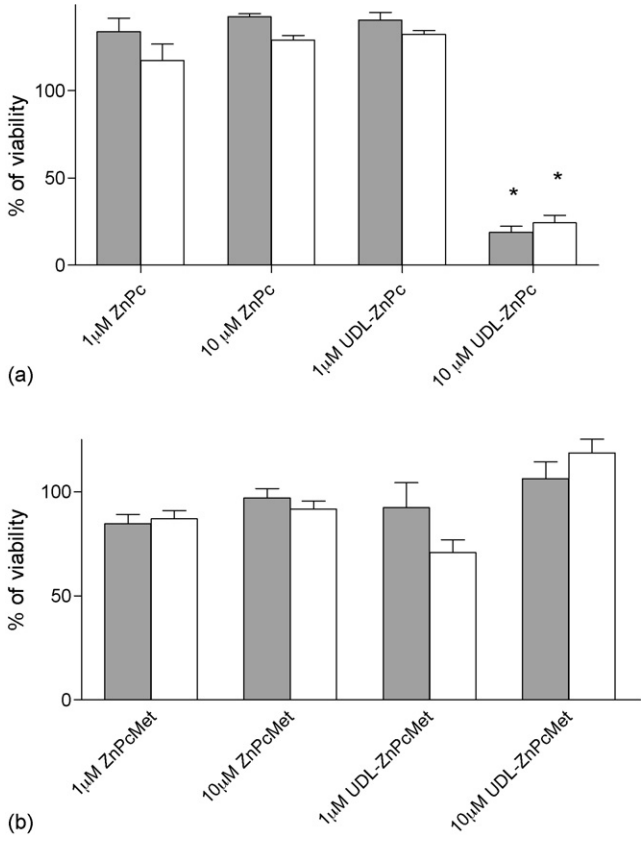

Fig. 7. Cytotoxicity of free and liposomal phthalocyanines in the dark (■) or upon irradiation (□) on J-774 cells: (a) ZnPc and (b) ZnPcMet. Each data point represents the mean ± standard deviation ($n = 3$). Student's t-test was used to compare statistical significance of treatments (differences: $^{*}p < 0.05$).

Table 3
Summary of ground excited state properties of free ZnPc and ZnPcMet in ethanol and buffer, respectively, and incorporated in liposomes

	Concentration (M)	λ_{max} (nm)	$\varepsilon_{\lambda_{max}}$ (M^{-1} cm^{-1})	Φ_F	Φ_Δ
Free ZnPc (ethanol)	3.47×10^{-7}	707	1.00×10^{6}	0.20 ± 0.03	0.80 ± 0.16
Free ZnPcMet (buffer)	1.06×10^{-6}	702	2.21×10^{4}	0.11 ± 0.02	0.21 ± 0.04
UDL-ZnPc	9.52×10^{-8}	707	1.16×10^{6}	0.20 ± 0.04	0.61 ± 0.12
UDL-ZnPcMet	1.40×10^{-7}	701	5.32×10^{5}	0.20 ± 0.04	0.79 ± 0.16

3.6. Liposomal cell uptake and fate of liposomal HPTS upon irradiation

Excitation spectrum of HPTS (350–450 nm) is highly sensitive to pH, whereas its emission spectrum (510 nm) is invariant. When HPTS/DPX containing liposomes are captured by cells and as long as they remain intact inside the endo/phago/lysosomes or if HPTS is released inside those acid compartments, a poorly visible fluorescence is registered under blue excitation. In contrast, HPTS release in a neutral-pH compartment such as the cytoplasm is recorded as intense fluorescence filling the whole cell (Straubinger, 1993).

a. Liposomal cell uptake (pulse and chase): only J-774 cells showed fluorescence after 5 min incubation, whereas Vero cells requiered at least an incubation of 15 min to show any signal. The first minute after 15 min incubation, Vero cells showed peripheric fluorescence (Fig. 8a), whereas J-774 cells already presented the whole perinuclear zone filled with green fluorescence (Fig. 8b). After nearly 45 min, fluorescent vesicular compartments appeared in the cytoplasm of Vero cells, while peripheric fluorescence remained present; no changes were registered on signals from J-774 cells along the same time period. The longer onset for liposomal uptake and the slower transit from periphery towards the perinuclear zone, indicated that Vero cells captured and processed the fluorescent UDL at a much slower rate than J-774 cells.

Intracellular co-localization in Vero (Fig. 8c and d) and J-744 cells (Fig. 8e and f) of both phthalocyanines (red fluorescence; Fig. 8c and e) and HPTS (green fluorescence;

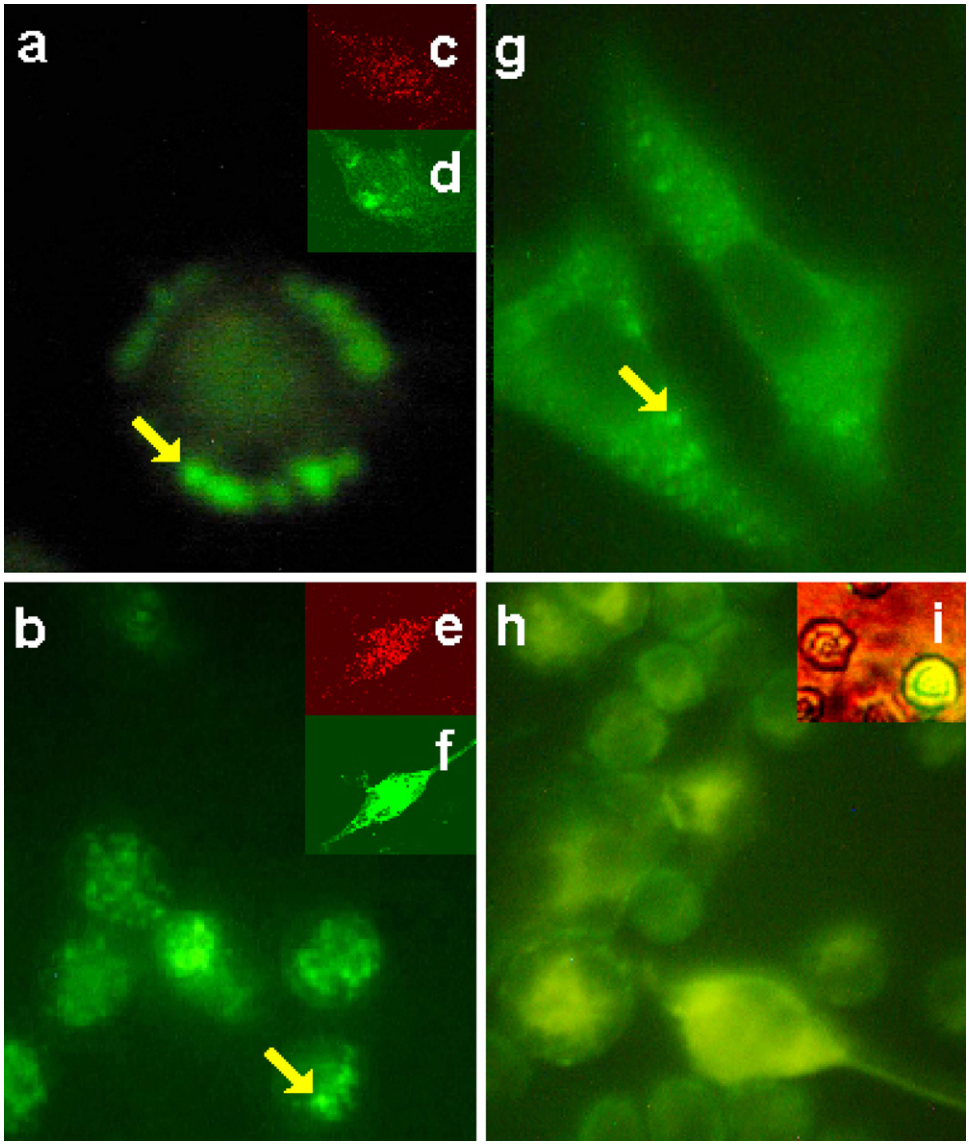

Fig. 8. Fluorescence microscopy images of Vero (a) and J-774 cells (b) upon 15 min incubation in the dark with UDL-HPTS/DPX. Confocal fluorescence microscopy of Vero (c and d) and J-774 (e and f) upon 45 min in the dark with UDL-HPTS/DPX-ZnPcMet showing phthalocyanine distribution in red (c and e) and HPTS in green (d and f), z-axis deep 5 μm. Vero (g) and J-744 cells (h) upon 45 min incubation in the dark followed by 30 min irradiation. (i) HPTS release into the cytoplasm of J-774 cells by pH-sensitive liposomes. Arrows show vesicular fluorescence. (For interpretation of the references to color in this figure legend, the reader is referred to the web version of the article.)

Fig. 8d and f) upon 45 min incubation (a time period long enough to allow uptake and processing of UDL by the two cell lines) in the dark with liposomal phthalocyanines (UDL-HPTS/DPX-ZnPc//-ZnPcMet) was revealed by sequential *z*-axis confocal microscopy images.

b. Fate of liposomal HPTS: effect of phthalocyanines and effect of irradiation: no changes in pale vesicular fluorescence on Vero cells cytoplasms, nor perinuclear brightness on J-774 cells incubated with UDL-HPTS/DPX were registered upon 30 min irradiation.

On the other hand, liposomal phthalocyanines (UDL-HPTS/DPX-ZnPc//-ZnPcMet) did not induce changes in HPTS signal distribution upon 30 min irradiation both on Vero (Fig. 8g) and J-774 cells (Fig. 8h). Additionally, the two different liposomal phthalocyanines produced no differences on HPTS signal on each cell line.

4. Discussion

To be used for PDT, a phthalocyanine derivative must have long wavelength absorption in the red region of the visible spectrum to achieve deeper penetration in biological tissues (Yarmush et al., 1993), high molar extinction coefficient (ε) and photostability. The singlet molecular oxygen generated by these sensitizers upon light absorption, is the reactive species responsible for the antitumor or antimicrobial activity (Ben-Hur and Rosenthal, 1985). Zinc and aluminium phthalocyanines have been extensively studied for PDT purposes, not only due to their high triplet quantum yields and long triplet lifetimes that lead to high Φ_Δ but also for their low Φ_F (Paquette and van Lier, 1992). From a photochemical point of view, design of liposomal photosensitizers is aimed to increase the monomer concentration and therefore the Φ_Δ in aqueous media. From a structural point of view, elastomechanical properties of UDL used in this study obey to precise combinations of three components; a fourth component could shift that equilibrium, inducing non-lamellar phases or non-UD bilayers (Almgren, 2000). Hence, impact of the hydrophobic and hydrophilic phthalocyanine derivatives on lamellar phase stability and ultradeformability, and the determination of the liposomal monomer state, conformed the initial part of this work.

The incorporation of photosensitizers to liposomes has been faced with variable outcome in terms of dimer/monomer equilibrium shift. Previous reports indicate that ZnPc has been loaded in liposomes by the ethanolic injection method to get up to 5 μM in the monomer form (Oliveira et al., 2005). Hydrophobic porphyrins derivates (Postigo et al., 2004), hypocrellin B (Yu et al., 2001) and photofrin (Sadzuka et al., 2005) were loaded in liposomes by hydration of a thin film to get monomer forms of non-reported concentration, but with lower Φ_Δ than those obtained in organic solvent for porphyrins derivates and hypocrellin B, although higher than that obtained of photofrin in aqueous media. The simple addition of the porphyrin derivative chlorine (Das et al., 2005) or an octasubstituted ZnPC (Rodriguez et al., 2003) to preformed liposomes renders aggregates at 6.7 and 2.7 μM, respectively. Our results indicate that employing the method of hydration of the thin film plus extrusion it is possible to incorporate hydrophobic and hydrophilic phthalocyanine derivatives in 100 nm unilamellar vesicles of low polydispersity with high Zeta potential and colloidal stability for at least 30 days. Liposomal ZnPc not only allowed to make ZnPc soluble in aqueous buffer, but also had a Φ_Δ almost equal to that obtained in organic solvent, indicating that the monomer form was present. On the other hand, as judged by its absorption spectra and low Φ_Δ value, free ZnPcMet aggregated at 0.01 μM in buffer; however, 0.1 μM liposomal ZnPcMet rendered a four-fold higher Φ_Δ when compared to that of the free form. As a remarkable advantage, liposome can be submitted to dialysis or lyophilization, enabling a further increase of the monomer concentration in the whole dispersion. A wide range of molecules (from low MW steroids to peptides and proteins) has recently been loaded into UDL (Cevc et al., 1998; Hofer et al., 1999; El Maghraby et al., 2000; Cevc and Blume, 2001, 2003, 2004; Essa et al., 2002; Fesq et al., 2003; Simoes et al., 2004; Fang et al., 2006); photosensitizers, on the other hand, have also been incorporated into conventional liposomes (Decreau et al., 1999; Namiki et al., 2004; Takeuchi et al., 2004; Liu et al., 2005; Rancan et al., 2005; Magaraggia et al., 2006). This is however, the first report where photosensitizers are incorporated to UDL.

ΔH_{cal} determined by DSC of ultradeformable matrices showed that ZnPc inserted in depth and magnitude strong enough to almost eliminate the bilayer transition cooperativity. However, neither the ZnPc insertion nor the lower interaction of ZnPcMet affected the ultradeformability, that resulted in the order of that found by van den Bergh (van den Bergh et al., 2001). The leakage of inner aqueous content when submitted to an extrusion stress – another typical feature of ultradeformable matrices – was neither affected by the presence of ZnPc nor by ZnPcMet, resulting three-fold lower than that of conventional liposomes. The post-stress quantification of ZnPc showed no relevant lost from liposomes; while only a minor quantity of ZnPcMet was lost, comparable to the amount of HPTS leakage. In the deformability test showed in this work, only the ultradeformable (UD) liposomes could pass through two 50 nm polycarbonate membranes upon applying an external pressure of 0.8 MPa; in those conditions, the measured phospholipid flux was indicative of the liposome ultradeformability. *In vivo* however, the transdermal hydration gradient that physiologically exists (nearly from 15% relative humidity on the skin surface to 70% in the basal layer), provides – even in the absence of an external pressure – the driving force for highly hydrated vesicles to move toward more hydrated deeper layers (Rama Krishna and Marsh, 1990; Seddon et al., 1990). It is also known that this enforces widening of the weakest intercellular junctions in the barrier and creates 20–30 nm-wide transcutaneous channels (Heimburg et al., 1990). It is important to understand that any hydrated vesicle on the skin surface will experience such force, but only the UD liposomes, due to their particular elastomechanical properties, can effectively make use of it to move across hydrophilic nanochannels without fusing nor coalesce. Because of this, it is not necessary any clinical device to force the penetration of the UD liposomes; moreover, their application must not be mediated by occlusive patches, since in those conditions the hydration

gradient – and therefore the driving force – is dissipated (Cevc and Gebauer, 2003)

Advantages of PDT in comparison to conventional antimicrobial chemotherapy are the lack of selection of PDT resistant strains even after multiple treatments (Nitzan et al., 1994; Calzavara-Pinton et al., 2005) and the low cost of photosensitizers that make PDT suitable to be implemented in poorly funded healthcare systems (e.g. in the developing world). It is already known that *Leishmania* amastigotes are sensitive to PDT with phthalocyanine derivatives; however, that sensitivity could be increased by means of a controlled release system. As it was suggested in a recent work (Dutta et al., 2005), both promastigotes and axenic amastigotes from *Leishmania amazonensis* were more sensitive than J-774 mammal cells to PDT with AlPhCl (aluminum phtalocyanine chloride), achieving cytolisis at low concentrations (~1 μM) and low light doses (1.5 J/cm^2). However, those results could only be achieved when AlPhCl pre-treated amastigotes were used to infect J-774 cells and not if infected cells were treated with AlPhCl. Clearly, the impaired delivery of photosensitizer to the intracellular target is responsible for a limitation of those experimental results, even in the absence of SC as a permeability barrier and without selectivity requirements. Because of that, a delivery strategy for topical application against cutaneous leishmaniasis has to be designed on account of the complex anatomical environment imposed by four three-dimensional barriers: (a) the SC, (b) the cell membrane of infected cells, (c) the vacuole membrane of amastigote and (d) the amastigote membrane. An adequate intracellular distribution is also pursued: inside the cells, co-localization or confinement of photosensitizers and therapeutic target in a small volume is required, due to the short lifetime (<0.1 ms) and short range of action (10–20 nm) of $^1O_2$ (Moan and Berg, 1991). As compared to the abundant studies on the intracellular effects caused by free photosensitizers, there is less information on the effect of conventional liposomal photosensitizers, and no data on UDL photosensitizers. Because of that, the second part of this *in vitro* study started by screening for potential toxic effects. Finally, since vesicular structures (primary, secondary, recycling endosomes, lisosomes) mediate the uptake mechanisms and further processing of liposomes, the vesicular traffic, revealed by HPTS/DPX, was followed before and after irradiation. We found that cytotoxicity, as measured by the MTT assay on Vero and J-774 cell lines, was absent for free phthalocyanines up to 10 μM, as well as for empty UDL up to 18 mM, both in dark or after sunlight irradiation. Also, liposomal phthalocyanines were not toxic on Vero cells, in both conditions. Conversely, viability of J-774 cells was reduced (75%) only upon UDL-ZnPC treatment at 10 μM, both in dark or after sunlight irradiation. This indicated that cytotoxicity was concentration, cell line and liposomal phthalocyanine type dependent.

The epidermis is a complex series of cells strata and amastigotes infect phagocytic cells (skin macrophages and dendritic cells) of impaired access from the deeper layers. Because of that, it was our interest to determine the impact caused by UDL photosensitizers on J-774 cells, of similar characteristics to those naturally infected. Differences on intrinsic metabolic activity and uptake rate of particulate material between J-774 and Vero cells were depicted as different HPTS patterns before irradiation. While J-774 cells specialize in the uptake (higher than that of soluble material) and rapid processing of particulate material (Hackam et al., 1998; Cox et al., 2000), Vero cells specialize in the endocytosis of soluble material (Conner and Schmid, 2003). The evolution of fluorescence patterns followed along nearly 1 h confirmed that J-774 cells were more capable of faster and massive uptake of ultradeformable liposomes than Vero cells. On the other hand, after irradiation at 15 J/cm^2 energy density (corresponding to the media energy provided by 15 min exposure at noon at southern latitude), we found that none free or liposomal phthalocyanines, could induce intracellular changes in HPTS signal on both cell lines. According to our results, the invariant HPTS signal corresponded to that of HPTS confined inside acid vesicles. This is supported by comparison with the massive bright shown by a J-774 cell (Fig. 8i), produced upon the uptake of pH-sensitive liposomes loaded with HPTS/DPX pair, and release of HPTS to cytoplasm. The phenomenon known as photochemical internalisation (PCI) (Berg and Moan, 1994; Moan et al., 1994; Høgset et al., 2004) occurs upon light exposition on cells containing photosensitizers in their endocytic vesicles, with permeabilization of the vesicles and release of the photosensitizer, together with unrelated molecules (proteins or nucleic acids, for example) located inside the endosomes or lysosomes. PCI can occur without inducing extensive cell death (Berg and Moan, 1994) and with maintenance of the biological activity of the released molecule. In our case, liposomal photosensitizers were located inside the endosomes, since phagocytosis and endocytosis were the only mechanisms that cells employ for liposomal uptake. However, a potential PCI could be discarded since the photosensitizers are not inserted in the endosomal bilayer, but soluble in the liposomal inner aqueous space or partitioned in the liposomal bilayer. On the other hand, PCI has only been registered for low aggregated amphipatic photosensitizers that partition in the endosomal membrane, such as the hydrophilic moiety points to the endosomal lumen (Prasmickaite et al., 2001). Therefore, the lack of PCI for free phthalocyanines could be ascribed to the aqueous solubility of ZnPcMet and to the high hydrophobicity of ZnPc.

In sum, those results have revealed that UDL could be loaded at high concentrations of hydrophobic or hydrophilic photosensitizers in monomeric state, which did not perturb the matrix ultradeformability. The higher capacity of J-774 cells for the uptake of UDL photosensitizers in the absence of toxicity even at high concentrations could contribute, once *in vivo*, to increase a passive targeting to infected cells. Additionally, it could be expected that the maintenance of endo-lisosomal structure as judged by the absence of PCI upon irradiation, should allow the *Leishmania* amastigotes and photosensitizer to be confined within the endo-lisosomal system, thereby increasing the phototoxic effect over the parasites.

Although further *in vivo* studies will be required to confirm these *in vitro* first steps in designing a strategic tool capable of crossing structural barriers, our results allow to propose the UD photosensitizers as potential topical agents for PDT against early cutaneous leishmaniasis.

Acknowledgements

This research was supported by a grant from Secretaría de Investigaciones, Universidad Nacional de Quilmes. F. Doctorovich, L. Dicelio, M.J. Morilla and E.L. Romero are members of the Carrera de Investigador del Consejo Nacional de Investigaciones Científicas y Técnicas (CONICET, Argentina). J. Montanari has got a fellowship from CONICET, Argentina. The authors wish to thank to Drs. Manel Sabes Xamani and Joan Estelrich from the Universitat Autónoma de Barcelona and Universitat de Barcelona, España, for the electronic microscopies as well as vesicle size and *Z*-potential measurements.

References

Abok, K., Cadenas, E., Brunk, U., 1988. An experimental model system for leishmaniasis. Effects of porphyrin-compounds and menadione on *Leishmania* parasites engulfed by cultured macrophages. Apmis 96, 543–551.

Abraham, W., Downing, D.T., 1990. Interaction between corneocytes and stratum corneum lipid liposomes in vitro. Biochim. Biophys. Acta 1021, 119–125.

Almgren, M., 2000. Mixed micelles and other structures in the solubilization of bilayer lipid membranes by surfactants. Biochim. Biophys. Acta 1508, 146–163.

Barry, B.W., 2001. Novel mechanisms and devices to enable successful transdermal drug delivery. Eur. J. Pharm. Sci. 14, 101–114.

Ben-Hur, E., Rosenthal, I., 1985. The phthalocyanines: a new class of mammalian cells photosensitizers with a potential for cancer phototherapy. Int. J. Radiat. Biol. Relat. Stud. Phys. Chem. Med. 47, 145–147.

Berg, K., Moan, J., 1994. Lysosomes as photochemical targets. Int. J. Cancer 59, 814–822.

Blank, I.H., Scheuplein, R.J., 1969. Transport into and within the skin. Br. J. Dermatol., 4–10.

Blum, J., Desjeux, P., Schwartz, E., Beck, B., Hatz, C., 2004. Treatment of cutaneous leishmaniasis among travelers. J. Antimicrob. Chemother. 53, 158–166.

Bötcher, C.J.F., Van Gent, C.M., Pries, C., 1961. A rapid and sensitive sub-micro phosphorus determination. Anal. Chim. Acta 24, 203–204.

Calzavara-Pinton, P.G., Venturini, M., Sala, R., 2005. A comprehensive overview of photodynamic therapy in the treatment of superficial fungal infections of the skin. J. Photochem. Photobiol. B 78, 1–6.

Cevc, G., 1995. In: Lipowsky, R.S.E. (Ed.), Handbook of Biological Physics. Elsevier, Amsterdam, pp. 465–490.

Cevc, G., 1996. Transfersomes, liposomes and other lipid suspensions on the skin: permeation enhancement, vesicle penetration, and transdermal drug delivery. Crit. Rev. Ther. Drug Carrier Syst. 13, 257–388.

Cevc, G., 2004. Lipid vesicles and other colloids as drug carriers on the skin. Adv. Drug Deliv. Rev. 56, 675–711.

Cevc, G., Blume, G., 1992. Lipid vesicles penetrate into intact skin owing to the transdermal osmotic gradients and hydration force. Biochim. Biophys. Acta 1104, 226–232.

Cevc, G., Blume, G., 2001. New, highly efficient formulation of diclofenac for the topical, transdermal administration in ultradeformable drug carriers, transfersomes. Biochim. Biophys. Acta 1514, 191–205.

Cevc, G., Blume, G., 2003. Biological activity and characteristics of triamcinolone-acetonide formulated with the self-regulating drug carriers, transfersomes. Biochim. Biophys. Acta 1614, 156–164.

Cevc, G., Blume, G., 2004. Hydrocortisone and dexamethasone in very deformable drug carriers have increased biological potency, prolonged effect, and reduced therapeutic dosage. Biochim. Biophys. Acta 1663, 61–73.

Cevc, G., Gebauer, D., 2003. Hydration-driven transport of deformable lipid vesicles through fine pores and the skin barrier. Biophys. J. 84, 1010–1024.

Cevc, G., Gebauer, D., Stieber, J., Schatzlein, A., Blume, G., 1998. Ultraflexible vesicles, transfersomes, have an extremely low pore penetration resistance and transport therapeutic amounts of insulin across the intact mammalian skin. Biochim. Biophys. Acta 1368, 201–215.

Cevc, G., Schätzlein, A., Gebauer, D., Blume, G., 1993. In: Bain, K.R., Hadgkraft, J., James, W.J., Water, K.A. (Eds.), Prediction of Percutaneous Penetration, vol. 3b. STS Publishing, Cardiff, pp. 226–234.

Conner, S.D., Schmid, S.L., 2003. Regulated portals of entry into the cell. Nature 422, 37–44.

Cox, D., Lee, D.J., Dale, B.M., Calafat, J., Greenberg, S., 2000. A Rab11-containing rapidly recycling compartment in macrophages that promotes phagocytosis. Proc. Natl. Acad. Sci. U.S.A. 97, 680–685.

Das, K., Dube, A., Gupta, P.K., 2005. A spectroscopy study of photobleaching of chlorin p6 in different environments. Dyes Pigments, 201–205.

De Filippis, M.P., Fantetti, D.D., Roncucci, L., 2000. Synthesis of a new water-soluble octa-cationic phthalocyanine derivative for PDT. Tetrahedron Lett. 41, 9143–9147.

Decreau, R., Richard, M.J., Verrando, P., Chanon, M., Julliard, M., 1999. Photodynamic activities of silicon phthalocyanines against achromic M6 melanoma cells and healthy human melanocytes and keratinocytes. J. Photochem. Photobiol. B 48, 48–56.

Dutta, S., Ray, D., Kolli, B.K., Chang, K.P., 2005. Photodynamic sensitization of *Leishmania amazonensis* in both extracellular and intracellular stages with aluminum phthalocyanine chloride for photolysis in vitro. Antimicrob. Agents Chemother. 49, 4474–4484.

El Maghraby, G.M., Williams, A.C., Barry, B.W., 2000. Oestradiol skin delivery from ultradeformable liposomes: refinement of surfactant concentration. Int. J. Pharm. 196, 63–74.

Enk, C.D., Fritsch, C., Jonas, F., Nasereddin, A., Ingber, A., Jaffe, C.L., Ruzicka, T., 2003. Treatment of cutaneous leishmaniasis with photodynamic therapy. Arch. Dermatol. 139, 432–434.

Essa, E.A., Bonner, M.C., Barry, B.W., 2002. Iontophoretic estradiol skin delivery and tritium exchange in ultradeformable liposomes. Int. J. Pharm. 240, 55–66.

Fang, J.Y., Hwang, T.L., Huang, Y.L., Fang, C.L., 2006. Enhancement of the transdermal delivery of catechins by liposomes incorporating anionic surfactants and ethanol. Int. J. Pharm. 310, 131–138.

Fernandez, D.A., Awruch, J., Dicelio, L.E., 1996. Photophysical and aggregation studies of *t*-butyl substituted Zn phthalocyanines. Photochem. Photobiol. 63, 784–792.

Fernandez, D.A., Dicelio, L.E., Awruch, J., 1995. Synthesis of two new *N*-alkyl substituted phthalocyanines. J. Heterocycl. Chem. 32, 519–522.

Fesq, H., Lehmann, J., Kontny, A., Erdmann, I., Theiling, K., Rother, M., Ring, J., Cevc, G., Abeck, D., 2003. Improved risk-benefit ratio for topical triamcinolone acetonide in transfersome in comparison with equipotent cream and ointment: a randomized controlled trial. Br. J. Dermatol. 149, 611–619.

Fry, D.W., White, J.C., Goldman, I.D., 1978. Rapid separation of low molecular weight solutes from liposomes without dilution. Anal. Biochem. 90, 809–815.

Gardlo, K., Horska, Z., Enk, C.D., Rauch, L., Megahed, M., Ruzicka, T., Fritsch, C., 2003. Treatment of cutaneous leishmaniasis by photodynamic therapy. J. Am. Acad. Dermatol. 48, 893–896.

Hackam, D.J., Rotstein, O.D., Sjolin, C., Schreiber, A.D., Trimble, W.S., Grinstein, S., 1998. v-SNARE-dependent secretion is required for phagocytosis. Proc. Natl. Acad. Sci. U.S.A. 95, 11691–11696.

Heimburg, T., Ryba, N.J., Wurz, U., Marsh, D., 1990. Phase transition from a gel to a fluid phase of cubic symmetry in dimyristoylphosphatidylcholine/myristic acid (1:2, mol/mol) bilayers. Biochim. Biophys. Acta 1025, 77–81.

Hofer, C., Gobel, R., Deering, P., Lehmer, A., Breul, J., 1999. Formulation of interleukin-2 and interferon-alpha containing ultradeformable carriers for potential transdermal application. Anticancer Res. 19, 1505–1507.

Hofland, H.E., Bouwstra, J.A., Bodde, H.E., Spies, F., Junginger, H.E., 1995. Interactions between liposomes and human stratum corneum in vitro: freeze fracture electron microscopical visualization and small angle X-ray scattering studies. Br. J. Dermatol. 132, 853–866.

Høgset, A., Prasmickaite, L., Selbo, P.K., Hellum, M., Engesaeter, B.O., Bonsted, A., Berg, K., 2004. Photochemical internalisation in drug and gene delivery. Adv. Drug Deliv. Rev. 56, 95–115.

Honeywell-Nguyen, P.L., Bouwstra, J.A., 2005. Vesicles as tool for transdermal and dermal delivery. Drug Discovery Today: Technol. 2, 67–74.

Hongcharu, W., Taylor, C.R., Chang, Y., Aghassi, D., Suthamjariya, K., Anderson, R.R., 2000. Topical ALA-photodynamic therapy for the treatment of acne vulgaris. J. Invest. Dermatol. 115, 183–192.

Kraljic, I., El Mohsni, S., 1978. A new method for the detection of singlet oxygen in aqueous solutions. Photochem. Photobiol. 28, 577–581.

Krieg, R.C., Messmann, H., Schlottmann, K., Endlicher, E., Seeger, S., Scholmerich, J., Knuechel, R., 2003. Intracellular localization is a cofactor for the phototoxicity of protoporphyrin IX in the gastrointestinal tract: in vitro study. Photochem. Photobiol. 78, 393–399.

Lagorio, M.G., Dicelio, L.E., San Román, E., 1993. Visible and near-IR spectroscopic and photochemical characterization of substituted metallophthalocyanines. J. Photochem. Photobiol. A 72, 153–161.

Lang, K., Lehmann, P., Bolsen, K., Ruzicka, T., Fritsch, C., 2001. Aminolevulinic acid: pharmacological profile and clinical indication. Expert Opin. Investig. Drugs 10, 1139–1156.

Liu, W., Jensen, T.J., Fronczek, F.R., Hammer, R.P., Smith, K.M., Vicente, M.G., 2005. Synthesis and cellular studies of nonaggregated water-soluble phthalocyanines. J. Med. Chem. 48, 1033–1041.

Liu, W., Lee, C., Chen, H., Mak, T.C.W., Ng, D.K.P., 2004. Synthesis, spectroscopic properties, and structure of tetrakis(24-dimethyl-3-pentyloxy)-phthalocyaninato metal complexes. Eur. J. Inorg. Chem., 286–292.

Magaraggia, M., Visona, A., Furlan, A., Pagnan, A., Miotto, G., Tognon, G., Jori, G., 2006. Inactivation of vascular smooth muscle cells photosensitised by liposome-delivered Zn(II)-phthalocyanine. J. Photochem. Photobiol. B 82, 53–58.

Menon, G.K., 2002. New insights into skin structure: scratching the surface. Adv. Drug Deliv. Rev. 54, S3–S17.

Moan, J., Berg, K., 1991. The photodegradation of porphyrins in cells can be used to estimate the lifetime of singlet oxygen. Photochem. Photobiol. 53, 549–553.

Moan, J., Berg, K., Anholt, H., Madslien, K., 1994. Sulfonated aluminium phthalocyanines as sensitizers for photochemotherapy. Effects of small light doses on localization, dye fluorescence and photosensitivity in V79 cells. Int. J. Cancer 58, 865–870.

Namiki, Y., Namiki, T., Date, M., Yanagihara, K., Yashiro, M., Takahashi, H., 2004. Enhanced photodynamic antitumor effect on gastric cancer by a novel photosensitive stealth liposome. Pharmacol. Res. 50, 65–76.

Nitzan, Y., Wexler, H.M., Finegold, S.M., 1994. Inactivation of anaerobic bacteria by various photosensitized porphyrins or by hemin. Curr. Microbiol. 29, 125–131.

Ochsner, M., 1997. Photophysical and photobiological processes in the photodynamic therapy of tumours. J. Photochem. Photobiol. B 39, 1–18.

Oliveira, C.A., Machado, A.E., Pessine, F.B., 2005. Preparation of 100 nm diameter unilamellar vesicles containing zinc phthalocyanine and cholesterol for use in photodynamic therapy. Chem. Phys. Lipids 133, 69–78.

Paquette, B., van Lier, J.E., 1992. In: Dougherty, B.W.H.A.T.J. (Ed.), Photodynamic Therapy. Marcel Dekker, New York, p. 195.

Postigo, F., Mora, M., De Madariaga, M.A., Nonell, S., Sagrista, M.L., 2004. Incorporation of hydrophobic porphyrins into liposomes: characterization and structural requirements. Int. J. Pharm. 278, 239–254.

Prasmickaite, L., Høgset, A., Berg, K., 2001. Evaluation of different photosensitizers for use in photochemical gene transfection. Photochem. Photobiol. 73, 388–395.

Rama Krishna, Y.V., Marsh, D., 1990. Spin label ESR and ^{31}P NMR studies of the cubic and inverted hexagonal phases of dimyristoylphosphatidylcholine/myristiic acid (1:2, mol/mol) mixtures. Biochim. Biophys. Acta 1024, 89–94.

Rancan, F., Wiehe, A., Nobel, M., Senge, M.O., Omari, S.A., Bohm, F., John, M., Roder, B., 2005. Influence of substitutions on asymmetric dihydroxychlorins with regard to intracellular uptake, subcellular localization and photosensitization of Jurkat cells. J. Photochem. Photobiol. B 78, 17–28.

Rodriguez, M.E., Moran, F., Bonansea, A., Monetti, M., Fernandez, D.A., Strassert, C.A., Rivarola, V., Awruch, J., Dicelio, L.E., 2003. A comparative study of the photophysical and phototoxic properties of octakis(decyloxy)phthalocyaninato zinc(II), incorporated in a hydrophilic polymer, in liposomes and in non-ionic micelles. Photochem. Photobiol. Sci. 2, 988–994.

Sadzuka, Y., Tokutomi, K., Iwasaki, F., Sugiyama, I., Hirano, T., Konno, H., Oku, N., Sonobe, T., 2005. The phototoxicity of photofrin was enhanced by PEGylated liposome in vitro. Cancer Lett..

Schatzlein, A., Cevc, G., 1998. Non-uniform cellular packing of the stratum corneum and permeability barrier function of intact skin: a high-resolution confocal laser scanning microscopy study using highly deformable vesicles (transfersomes). Br. J. Dermatol. 138, 583–592.

Scheuplein, R.J., Blank, I.H., 1971. Permeability of the skin. Physiol. Rev. 51, 702–747.

Seddon, J.M., Hogan, J.L., Warrender, N.A., Pebay-Peyroula, E., 1990. Structural studies of phospholipid cubic phases. Progr. Colloid Polym. Sci., 189–197.

Shigeo, F.Y.K., Toshihiro, M., Hiroyuki, S., Junichi, T., 1997. JP 9077731, Japan.

Simoes, S., Moreira, J.N., Fonseca, C., Duzgunes, N., de Lima, M.C., 2004. On the formulation of pH-sensitive liposomes with long circulation times. Adv. Drug Deliv. Rev. 56, 947–965.

Stojiljkovic, I., Evavold, B.D., Kumar, V., 2001. Antimicrobial properties of porphyrins. Expert Opin. Investig. Drugs 10, 309–320.

Strassert, C.A., Rodriguez, M.E., Fernandez, D.A., Dicelio, L.E., Awruch, J., 2003. Synthesis and properties of *N*-alkylsubstituted zinc(II) phthalocyaninates as potential agents for photodynamic therapy. Curr. Top. Med. Chem. 3, 165–173.

Straubinger, R.M., 1993. pH-sensitive liposomes for delivery of macromolecules into cytoplasm of cultured cells. Methods Enzymol. 221, 361–376.

Takeuchi, Y., Ichikawa, K., Yonezawa, S., Kurohane, K., Koishi, T., Nango, M., Namba, Y., Oku, N., 2004. Intracellular target for photosensitization in cancer antiangiogenic photodynamic therapy mediated by polycation liposome. J. Control. Release 97, 231–240.

Uriarte Cantolla, A., 2003 Historia del Clima de la Tierra. Servicio Central de Publicaciones del Gobierno Vasco.

van den Bergh, B.A., Wertz, P.W., Junginger, H.E., Bouwstra, J.A., 2001. Elasticity of vesicles assessed by electron spin resonance, electron microscopy and extrusion measurements. Int. J. Pharm. 217, 13–24.

Verma, D.D., Verma, S., Blume, G., Fahr, A., 2003. Liposomes increase skin penetration of entrapped and non-entrapped hydrophilic substances into human skin: a skin penetration and confocal laser scanning microscopy study. Eur. J. Pharm. Biopharm. 55, 271–277.

Weiner, N., Lieb, L., 1998. In: Papahadjopoulos (Ed.), Medical Applications of Liposomes. Elsevier Science B.V., pp. 493–510.

Wilkinson, F., Helman, W.P., Rose, A.D., 1995. Rate constant for the decay and reactions of the lowest electronically excited singlet state of molecular oxygen in solution. An expanded and revised compilation. J. Phys. Chem. Ref. Data 24, 663–1021.

Yarmush, M.L., Thorpe, W.P., Strong, L., Rakestraw, S.L., Toner, M., Tompkins, R.G., 1993. Antibody targeted photolysis. Crit. Rev. Ther. Drug Carrier Syst. 10, 197–252.

Yu, C., Chen, S., Zhang, M., Shen, T., 2001. Spectroscopic studies and photodynamic actions of hypocrellin B in liposomes. Photochem. Photobiol. 73, 482–488.